



On the Boundary Layer Flow of Ferrofluids



By

Muzammal Hameed Tariq

210-FBAS/MSMA/F-14

**Department of Mathematics and Statistics
Faculty of Basic and Applied Sciences
International Islamic University, Islamabad**

Pakistan

2016



ACCESSION NO

TH-16774 NY

K

ET

MS
S32 051
TAO

1. Boundary layer
2. Fluid dynamics

On the Boundary Layer Flow of Ferrofluids



By

Muzammal Hameed Tariq

Supervised by

Dr. Rahmat Ellahi

Department of Mathematics and Statistics

Faculty of Basic and Applied Sciences

International Islamic University, Islamabad

Pakistan

2016

On the Boundary Layer Flow of Ferrofluids

By

Muzammal Hameed Tariq

A Thesis

Submitted in the Partial Fulfillment of the
Requirements for the Degree of
MASTER OF PHILOSOPHY IN MATHEMATICS

Supervised by

Dr. Rahmat Ellahi

Department of Mathematics and Statistics

Faculty of Basic and Applied Sciences

International Islamic University, Islamabad

Pakistan

2016

Certificate

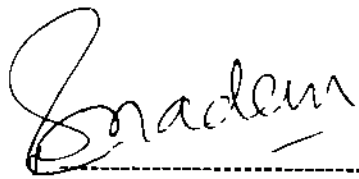
On the Boundary Layer Flow of Ferrofluids

By

Muzammal Hameed Tariq

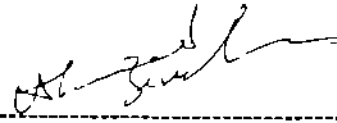
A THESIS SUBMITTED IN PARTIAL FULFILLMENT OF THE
REQUIREMENTS FOR THE DEGREE OF THE MASTER OF
PHILOSOPHY IN MATHEMATICS

We accept this as conforming to the required standard



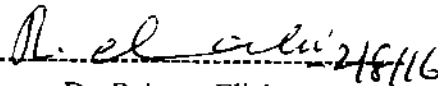
Prof Dr Sohail Nadeem
(External Examiner)

2



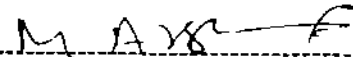
Dr Ahmad Zeeshan
(Internal Examiner)

3



Dr Rahmat Ellahi
(Supervisor)

4



Prof Dr Muhammad Arshad
(Chairman)

Department of Mathematics and Statistics

Faculty of Basic and Applied Sciences

International Islamic University, Islamabad

Pakistan

2016

Declaration

I hereby declare and affirm that this research work neither as whole nor as a part has been copied out from any source. It is further declare that I have developed this research work entirely on the basis of my personal efforts. If any part of this thesis is proven to be copied out or found to be a reproduction of some other, I shall stand by the consequences.

Moreover, no portion of the work presented in this thesis has been submitted in support of an application for other degree or qualification in this other university or institute of learning

Signature -----

Muzammal Hamced Tariq

M Phil Scholar (Mathematics)

210-FBAS/MSMA/F-14

Dedication

This thesis is dedicated to Holy prophet

Hazrat Muhammad (P.B.U.H)

&

My family

Acknowledgements

Primarily and foremost. I am thankful to Almighty Allah, who is the only creator and master of us, who created us from a clot and taught us to write with the pen who provided me the strength and ability to learn and to achieve another milestone to a destination. Countless droods and slams upoun prophet Muhammad (SAW) who is forever a torch of gaudiness, a source of knowledge and blessings for entire creation. His teaching shows us a way to live with dignity, stand with honor and learn to be humble.

Foremost thanks go to my supervisor **Dr. Rahmat Ellahi**, his dynamic supervision, guidance in a right direction, constant moral encouragements and motivation of hard work made my task easy and I completed my dissertation well within time. His comprehensive knowledge and logical way of thinking have been of greater value for me. His understanding, encouraging and personal guidance have provided a good basis to understand the field of fluid mechanics. His ideas and concepts have remarkable influence on my research skills. I have learned a lot from him.

I am much indebted to my senior research fellow **Dr. Mohsan Hassan** for his valuable advice in discussion, his precious time to guide and gave his comments. I truthfully acknowledge his for the ideas he enthusiastically shared with me to produce my best work. He really helped me out in every problem.

I am grateful to **Dr. Muhammad Arshad Zia**, Chairman Department of Mathematics for providing access to facilities that ensured successful completion of my work.

A warm thanks to **Mr. Shafee Ahmad, Mr. Ifraheem, Mr. Shoail, Mr. Amjad Mahmood, Mr. Awais and Mr. Bilal Arain**. Who offered me a lot of friendly help during my research work. Many thanks to **Dr. Ahmad Zeeshan, Dr. Nasir Ali, Dr. Mohsin Raza and Dr. Ahmar**, for their valuable discussions that helped me to understand my research area in much a better way.

Acknowledgements are incomplete without paying regards to my parents who've always given me perpetual love, care and cheers. Whose prayers have been a source of great inspiration for me and whose sustained hope in me led me to where I stand today. I have no words to thanks my Brothers **Tajamal Hameed Tariq, Hafiz Akmal Hameed Tariq** and Sisters who developed self-confidence and support me.

I am highly thankful to my relatives **Mr. Qasir Iqball, Mr. Haleem Khan, Mr. Jameel, Mr. Tajamal and Mr. Sajjad**. It is largely due to their efforts, moral supports and love that I am as I am today.

Muzammal Hameed Tariq
2nd August, 2016

Preface

On the boundary layer flow of ferrofluids are important in many processes. For instance, researchers have prepared ferrofluids, which have the fluid properties of a liquid and the magnetic properties of a solid. The ferrofluids actually contain tiny particles (~10 nm diameter) of a magnetic solid suspended in a liquid medium. Ferrofluids were originally discovered in the 1960s at the NASA research center, where scientists were investigating different possible methods of controlling liquids in space. The benefits of a magnetic fluid were immediately obvious. The location of the fluid could be precisely controlled through the application of a magnetic field and by varying the strength of the field, the fluids could be forced to flow. Researchers have prepared ferrofluids containing small particles of ferromagnetic metals, such as cobalt and iron, as well as magnetic compounds, like manganese zinc ferrite, $Zn_xMn_{1-x}Fe_2O_4$ ($0 < x < 1$; the family of solid solutions). But by far, the most work has been conducted on ferrofluids containing small particles of magnetite, Fe_3O_4 . One of many fascinating features of ferrofluid is the prospect of influencing flow by a magnetic field and vice-versa [1,2].

Moreover, ferrofluids have found a wide variety of applications, including use in rotating shaft seals. These rotating shaft seals are found in rotating anode X-ray generators and in vacuum chambers used in the semiconductor industry. Ferrofluid seals are used in high-speed computer disk drives to eliminate harmful dust particles or other impurities that can cause the data-reading heads to crash into the disks under engineering application.

The major application of ferrofluids in electrical field is improving the performance of loudspeakers. Finally, there is much hope for future biomedical applications of ferrofluids. For example, researchers are attempting to design ferrofluids that can carry medications to specific locations in the body through the use of applied magnetic fields. Ferrofluid have been investigated by a number of workers. Some recent investigations in this direction are presented in the refs [3-10].

In view of the above discussion the present dissertation is arranged as follows. Chapter one includes some relevant definitions and equations of the subsequent chapters.

Chapter two is a review work of [11]. In this paper the theoretical investigation of the effect of rotation on ferrofluid flow due to rotating disk by solving boundary layer equation is investigated. The couple of nonlinear differential equation have been

solved by power series approximations. Expressions for the components of velocity and pressure profile are obtained by cylindrical co-ordinate system by considering the z -axis as the axis of rotation. The results for all above variables are obtained numerically and discussed graphically.

Chapter three is the extension of chapter two in which the unsteady ferrofluid flow revolving a stretchable rotating disk on a boundary layer under the influence of low oscillating magnetic field is investigated. The governing partial differential equations are first converted into non-linear ordinary differential equations and then a convergent series solution is obtained using homotopy analysis method (HAM) [12-22]. Heat transfer analysis, velocity profile, pressure profile are discussed in the presence of particle concentration and magnetic isotropy. In addition, expression of Skin fraction, Nusselt number, angle between the wall and revolving ferrofluid, boundary layer thickness and volume flowing through the axial direction are discussed. Graphs are also presented to analyze the behavior of effective parameters on the velocity, temperature and pressure profiles.

Contents

1 Basic of fluid dynamic	3
1.1 Definition	3
1.1.1 Fluid	3
1.2 Types of fluids	3
1.2.1 Newtonian fluids	3
1.2.2 Non-Newtonian fluid	3
1.2.3 Ferrofluids	3
1.3 Magnetohydrodynamic (MHD)	4
1.3.1 Magnetism	4
1.3.2 Magnetic field	4
1.3.3 Magnetic permeability	4
1.3.4 Maxwell's equations	5
1.4 Force associate with fluid in motion	5
1.4.1 Force	5
1.4.2 Inertial force	5
1.4.3 Coriolis force	5
1.4.4 Centrifugal force	6
1.4.5 External force	6
1.4.6 Internal force	6
1.5 Heat transfer	6
1.5.1 Modes of heat flow	6
1.5.2 Conduction	7
1.5.3 Convection	7
1.5.4 Radiation	7
1.6 Physical description of dimensionless numbers	8
1.6.1 Reynolds number (Re)	8
1.6.2 Prandtl number (Pr)	8
1.6.3 Nusselt number (Nu)	8
1.6.4 Skin friction	9
2 On the revolving ferrofluid due to rotating disk	10

2 1	Mathematical formulation of the problem	10
2 1 1	Flow modelling	10
2 1 2	Parameters of physical interest	13
2 2	Solution of the problem	13
2 3	Results and discussion	16
2 4	Concluding remarks	20
3	On the boundary layer flow of ferrofluids	22
3 1	Mathematical formulation of the problem	22
3 1 1	Flow modelling	22
3 1 2	Thermodynamics properties	26
3 1 3	Parameters of physical interest	28
3 2	Solution of the problem	29
3 3	Results and discussion	31
3 4	Concluding remarks	36
	References	37

Chapter 1

Basic of fluid dynamic

This chapter comprises of some elementary definitions which may be useful for the better understanding of the next two chapters

1.1 Definition

1.1.1 Fluid

Any substance which shows resistance to its internal molecular structure when external force applies. Liquids and gases are identified as fluid since they deform continuously in response to shear stress.

1.2 Types of fluids

1.2.1 Newtonian fluid

Such fluid which obeys Newton's law of viscosity is called Newtonian fluid. Newton's law of viscosity is given by

$$\tau = \mu \frac{du}{dy} \quad (1.1)$$

Where, τ is the shear stress, μ is the viscosity of fluid, $\frac{du}{dy}$ is the shear rate or velocity of gradient. Gases and most common liquids are tends to Newtonian fluids. Most common examples are Water, thin motor oil, air, sugar solutions, silicone, etc.

1.2.2 Non-Newtonian fluids

Fluid which do not obey the Newton's law of viscosity's is called non-Newtonian fluid. Common examples are paints, flour dough, coal tar, ketchup, shampoo, chewing gum and fruit juice.

1.2.3 Ferrofluid

A ferrofluid is a liquid that becomes strongly magnetized in the presence of a magnetic field.



Fig. 1.1: Ferrofluid on glass with a magnet underneath

1.3 Magnetohydrodynamics (MHD)

MHD is a discipline which studies the dynamics of electrically conducting fluids. The word magnetohydrodynamics (MHD) is derived from magneto-meaning magnetic field, hydro-meaning liquid, and dynamics meaning movements. The field of MHD was initiated by Hannes Alfvén for which he received the Nobel prize in physics in 1970. Examples of such fluids include plasmas, liquid metal and seawater.

1.3.1 Magnetism

The study of nature, and cause of magnetic force fields and how different substances are affected by them is called magnetism.

1.3.2 Magnetic field

The region or space around a magnet in which it exerts a force on other magnet, is called its magnetic field. It is mostly strong near poles. The path of small magnet in a magnetic field is called magnetic field lines. The magnetic field is vector quantity and has SI unit of Tesla.

1.3.3 Magnetic permeability

This is the property of material that is equal to magnetic flux density B established within the material by magnetizing field divided by magnetic field strength H of the magnetizing field. Mathematically one can write it as

$$\mu_m = \frac{B}{H} \quad (1.2)$$

Where μ_m is the magnetic permeability

1.3.4 Maxwell's equations

The Maxwell's equations are the set of four fundamental equations governing electro-magnetism, i.e., the behavior of electro and magnetic fields. They were first written down in complete form by James Clerk Maxwell. For the varying fields the differential form of those equations in MKS are given as

$$\left. \begin{aligned} \nabla \cdot \mathbf{E} &= \frac{\rho}{\epsilon_0}, \\ \nabla \times \mathbf{E} &= -\frac{\partial \mathbf{B}}{\partial t}, \\ \nabla \cdot \mathbf{B} &= 0, \\ \nabla \times \mathbf{B} &= \mu_0 \mathbf{J} + \epsilon_0 \mu_0 \frac{\partial \mathbf{E}}{\partial t} \end{aligned} \right\} \quad (1.3)$$

Where \mathbf{E} is the electric field, \mathbf{B} is the magnetic field. \mathbf{J} is the charge density. $\epsilon_0 = 8.854187817 \times 10^{-12} \text{ Fm}^{-1}$ is the permittivity of free space and $\mu_0 = 1.2566370614 \times 10^{-6} \text{ NA}^{-2}$ is the permeability of free space.

1.4 Force associate with fluid in motion

1.4.1 Force

Force is defined as an action that alters or tends to alter a body's state of rest or uniform motion in a straight line. Its magnitude and direction is given by vector \mathbf{F} .

1.4.2 Inertial force

If several forces act on a particle of mass m and produced an acceleration \mathbf{a} , the magnitude F of the vector sum of applied forces is equal to $m\mathbf{a}$. Thus

$$\mathbf{F} - m\mathbf{a} = 0 \quad (1.4)$$

Where, $-m\mathbf{a}$ is called inertial force. Examples are the Coriolis force and the centrifugal force that appears in rotating coordinate system.

1.4.3 Coriolis force

The Coriolis force is an inertial force that acts on objects which are in motion relative to a rotating reference frame. In a reference frame with clockwise rotation, the force acts to the left of the motion of the object. In one with anticlockwise rotation, the force acts to the right. The Coriolis forces are always perpendicular to the direction of flow so the pressure gradient is also perpendicular to the flow.

The vector formula for the magnitude and direction of the Coriolis acceleration is

$$a_c = -2\Omega \times v \quad (1.5)$$

In above, a_c is the acceleration of the particle in the rotating system, v is the velocity of the particle with respect to the rotating system, Ω is the angular velocity vector of magnitude equal to the rotation rate ω directed along the axis of rotation in rotating reference frame of reference and the \times symbol represents the cross product operator

1.4.4 Centrifugal force

The term centrifugal force is refer to an inertial force directed away from the axis of rotation that appears to act on all objects when viewed in a rotating reference frame. The concept of centrifugal force can be applied in rotating devices such as centrifuges, centrifugal pumps and centrifugal governors etc

1.4.5 External force

A force applied at an element of area dA tends to distort some other element of area dB and is transmitted throughout the body. For example, body forces and surface forces. These forces are also called long-range forces.

1.4.6 Internal force

A force exerted by matter on one side to that on the other side is termed on internal force. One of its examples is stress. It can be resolved in to components normal and tangential to the area that are called tensile stress component and the shear stress component respectively. These forces are also called short-range forces.

1.5 Heat transfer

In physics, heat is the energy transferred from one body or system to another due to difference in temperature. The discipline of heat transfer is concerned with only two things one of them is temperature and the other is flow heat. Temperature represents the amount of thermal energy available, whereas, heat flow represent the movement of thermal energy from place to place.

1.5.1 Modes of heat flow

Modes of heat transfer are mainly classified into three categories as given below.

- i. Conduction
- ii. Convection
- iii. Radiation

1.5.2 Conduction

Conduction is a heat flow through solids without any visible movement of the particles. It is because of temperature difference in which heat transportations take place from the more energetic particles to energetic fluid particles only by collision or because of molecular vibrations and the energy movement by free electrons. Heat transfer occurs in Silver, Copper, Mercury and Iron through conduction. Heat conduction rate depends upon the medium's geometry, relative thickness and the type of material. It can be easily measured in one dimension as follows:

$$\text{Heat conduction rate} \propto \frac{(\text{area})(\text{temperature difference})}{\text{thickness}}, \quad (1.6)$$
$$Q_{\text{cond}} = k_f A \frac{T_1 - T_2}{\Delta x}$$

The above equation is also called heat conduction equation in which proportionality constant k_f stands for material's thermal conductivity which measures the material's heat conducting capability. When $\Delta x \rightarrow 0$ then the above equation becomes

$$Q_{\text{cond}} = -k_f A \frac{dt}{dx} \quad (1.7)$$

The above equality is recognized as Fourier's law of heat conduction.

1.5.3 Convection

Heat convection is the transportation and exchange of heat, due to mixing motion of different parts of fluid. It is governed by the laws of fluid dynamics in combination with the laws of heat conduction. Examples of convection are hot water, the cooling system of an automobile engine, the flow of the blood in human body etc.

1.5.4 Radiation

Radiation is heat transfer mechanism in which heat transfer takes place from any material through emission or absorption of electromagnetic waves. Especially radiation is significant during combustion processes where temperature is very high, but can also be favorable at room's temperature. The transfer of heat due to radiation can occur through gasses, fluids or a vacuum. Distinct from conductive and convective processes, heat transfer by radiative processes does not require to propagate any material.

1.6 Physical description of dimensionless numbers

1.6.1 Reynolds number (Re)

This dimensionless quantity estimates the correspondence of inertial forces by viscous forces. Reynolds number is used to characterize fluid behavior in the boundary layer flow. Mathematically, it is given by

$$Re = \frac{\rho u^2 l}{\mu u} = \frac{\rho u l}{\mu} = \frac{lu}{\nu} \quad (1.8)$$

Where u is the fluid velocity, μ is the dynamic viscosity, l is the characteristic length and ν is the kinematic viscosity. Laminar flow is characterized by low Reynolds numbers (Dominance of viscous forces) whereas turbulent flow is characterized by high Reynolds numbers (Dominance of inertial forces).

1.6.2 Prandtl number (Pr)

The Prandtl number is a dimensionless number approximating the ratio of momentum diffusivity and thermal diffusivity. Mathematically, it is expressed by the following relation

$$Pr = \frac{\text{Viscous diffusion rate}}{\text{Thermal diffusion rate}}, \quad (1.9)$$
$$Pr = \frac{\mu C_p}{k}$$

In heat transfer problem, the Prandtl number controls the relative thickness of the momentum and thermal boundary layer. When Pr is small it means that heat diffuses very quickly compared to the velocity (momentum). In above equation C_p is the specific heat.

1.6.3 Nusselt number

The convective to conductive heat transfer ratio across a boundary layer is referred to Nusselt number. In mathematical notation, it can be written as

$$Nu = \frac{h\Delta T}{K\Delta T} = \frac{hl}{k} \quad (1.10)$$

Here, Nu , h , l and k are the Nusselt number, heat transfer coefficient, characteristic length and thermal conductivity respectively.

1.6.4 Skin friction

When fluid and surface are in relative motion, the drag force exerted by fluid on surface in contact is called skin friction. It can be expressed as

$$C_f = \frac{\tau_w}{\frac{1}{2}\rho u^2} \quad (1.11)$$

In above, C_f , τ_w , ρ and u stand for the skin friction, wall shear stress, density and velocity of moving object respectively.

Chapter 2

On the revolving ferrofluids flow due to rotating disk

This chapter deals with review investigation of the effect of rotation on ferrofluid flow due to rotating disk by solving boundary layer equation [11] Here, the couple of nonlinear differential equation are solved by power series approximations Expressions for the components of velocity and pressure profile are obtained by cylindrical co-ordinate system by considering the z -axis as the axis of rotation It is observed that there is significant increment in the thickness of the boundary layer over rotating due to comparison to the ordinary case of viscous fluid flow without rotation

2.1 Mathematical formulation of the problem

2.1.1 Flow modelling

The flow is isotropic medium is considered to be study ($\partial/\partial t = 0$) and axi-symmetric ($\partial/\partial\theta = 0$) excluding the thermal effects. The fluid and ferrous particles have the same velocity The fluid and disk are assumed to be electrically non-conducting The whole system is rotating with angular velocity $\Omega = (0, 0, \Omega)$ along the vertical axis, which is taken z -axis as shown in Fig. 2.1.

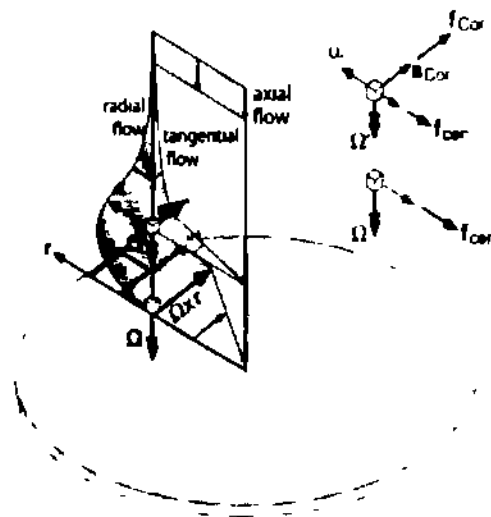


Fig. 2.1: Geometry of the problem

One additional simplification is assumed in momentum equation that the viscosity is independent of magnetic-field intensity. The continuity and momentum equations for incompressible ferromagnetic fluid with constant viscosity in a rotating frame of reference

$$\nabla \cdot \mathbf{V} = 0, \quad (2.1)$$

$$\rho \left[\frac{\partial \mathbf{V}}{\partial t} + (\mathbf{V} \cdot \nabla) \mathbf{V} \right] = -\nabla p + \mu_0 (\mathbf{M} \cdot \nabla) \mathbf{H} + \mu_f \nabla^2 \mathbf{V} + 2\rho (\boldsymbol{\Omega} \times \mathbf{V}) - \frac{\rho}{2} \nabla |\boldsymbol{\Omega} \times \mathbf{r}|^2 \quad (2.2)$$

In Eq (2.2) the effect of rotation includes Centrifugal force $-\frac{\rho}{2} \nabla |\boldsymbol{\Omega} \times \mathbf{r}|^2$ and

Coriolis acceleration $2\rho (\boldsymbol{\Omega} \times \mathbf{V})$. Here $P - \frac{\rho}{2} \nabla |\boldsymbol{\Omega} \times \mathbf{r}|^2 = p$ is the reduce pressure.

in which P stands for fluid pressure. The Maxwell's equations, simplified for a non-conducting fluid with no displacement currents are as follows

$$\nabla \times \mathbf{H} = 0, \quad \nabla \cdot (\mathbf{H} + 4\pi \mathbf{M}) = 0, \quad (2.3)$$

with assumptions

$$\mathbf{M} = \chi \mathbf{H}, \quad \chi = \frac{\mu_f}{\mu_0} - 1, \quad \mathbf{M} \times \mathbf{H} = 0 \quad (2.4)$$

Attentions have been drawn to the fact that the external magnetic field interacts with magnetic particles, not only through forces but also through couples. The velocity component v_z is less as compared to v_r and v_θ . The velocity components v_r , v_θ and v_z respectively along r , θ and z direction can be written as

$$\begin{aligned} & \frac{\partial v_r}{\partial t} + v_r \frac{\partial v_r}{\partial r} + \frac{v_\theta}{r} \frac{\partial v_r}{\partial \theta} + v_z \frac{\partial v_r}{\partial z} - \frac{v_\theta^2}{r} \\ & = F_r - \frac{1}{\rho} \frac{\partial p}{\partial r} + \nu \left[\frac{\partial^2 v_r}{\partial r^2} + \frac{1}{r} \frac{\partial v_r}{\partial r} + \frac{1}{r^2} \frac{\partial^2 v_r}{\partial \theta^2} + \frac{\partial^2 v_r}{\partial z^2} - \frac{v_r}{r^2} - \frac{2}{r^2} \frac{\partial v_\theta}{\partial \theta} \right], \end{aligned} \quad (2.5)$$

$$\begin{aligned} & \frac{\partial v_\theta}{\partial t} + v_r \frac{\partial v_\theta}{\partial r} + \frac{v_\theta}{r} \frac{\partial v_\theta}{\partial \theta} + v_z \frac{\partial v_\theta}{\partial z} - \frac{v_\theta^2}{r} \\ & = F_\theta - \frac{1}{\rho} \frac{\partial p}{\partial r} + \nu \left[\frac{\partial^2 v_\theta}{\partial r^2} + \frac{1}{r} \frac{\partial v_\theta}{\partial r} + \frac{1}{r^2} \frac{\partial^2 v_\theta}{\partial \theta^2} + \frac{\partial^2 v_\theta}{\partial z^2} - \frac{v_r}{r^2} - \frac{2}{r^2} \frac{\partial v_\theta}{\partial \theta} \right], \end{aligned} \quad (2.6)$$

$$\begin{aligned} \frac{\partial v_z}{\partial t} + v_r \frac{\partial v_z}{\partial r} + \frac{v_\theta}{r} \frac{\partial v_z}{\partial \theta} + v_z \frac{\partial v_z}{\partial z} \\ = F_z - \frac{1}{\rho} \frac{\partial p}{\partial z} + \nu \left[\frac{\partial^2 v_z}{\partial r^2} + \frac{1}{r} \frac{\partial v_z}{\partial r} + \frac{1}{r^2} \frac{\partial^2 v_z}{\partial \theta^2} + \frac{\partial^2 v_z}{\partial z^2} \right] \end{aligned} \quad (2.7)$$

Here $\partial/\partial t = 0$, $\partial/\partial \theta = 0$ and neglecting body force, the Eqs (2.5)-(2.7) are obtained as

$$\begin{aligned} v_r \frac{\partial v_r}{\partial r} + v_z \frac{\partial v_r}{\partial z} - \frac{v_\theta^2}{r} \\ = -\frac{1}{\rho} \frac{\partial p}{\partial r} + \frac{\mu_0}{\rho} |M| \frac{\partial}{\partial r} |H| + \nu \left[\frac{\partial^2 v_r}{\partial r^2} + \frac{\partial}{\partial r} \left(\frac{v_r}{r} \right) + \frac{\partial^2 v_r}{\partial z^2} \right] + 2\Omega v_\theta, \end{aligned} \quad (2.8)$$

$$v_r \frac{\partial v_\theta}{\partial r} + v_z \frac{\partial v_\theta}{\partial z} + \frac{v_r v_\theta}{r} = \nu \left[\frac{\partial^2 v_\theta}{\partial r^2} + \frac{\partial}{\partial r} \left(\frac{v_\theta}{r} \right) + \frac{\partial^2 v_\theta}{\partial z^2} \right] - 2\Omega v_r, \quad (2.9)$$

$$v_r \frac{\partial v_z}{\partial r} + v_z \frac{\partial v_z}{\partial z} = -\frac{1}{\rho} \frac{\partial p}{\partial z} + \frac{\mu_0}{\rho} |M| \frac{\partial}{\partial r} |H| + \nu \left[\frac{\partial^2 v_z}{\partial r^2} + \frac{1}{r} \frac{\partial v_z}{\partial r} + \frac{\partial^2 v_z}{\partial z^2} \right], \quad (2.10)$$

$$\frac{\partial v_r}{\partial r} + \frac{v_r}{r} + \frac{\partial v_z}{\partial z} = 0 \quad (2.11)$$

The associated initial and boundary condition for the flow due to rotation of an infinitely long disk ($z = 0$) with constant angular velocity ω are given by

$$\left. \begin{aligned} \text{at } z = 0, \quad v_r = 0, \quad v_\theta = r\omega, \quad v_z = 0 \\ \text{at } z \rightarrow \infty, \quad v_r = 0, \quad v_\theta = 0 \end{aligned} \right\} \quad (2.12)$$

Using the boundary layer approximation $-\frac{1}{\rho} \frac{\partial p}{\partial r} + \frac{\mu_0}{\rho} |M| \frac{\partial}{\partial r} |H| = -r\omega^2$ [23] with very less variation of magnetic-field in z-direction along with the following transformations

$$v_r = r\omega E(\alpha), \quad v_\theta = r\omega F(\alpha), \quad v_z = r\omega G(\alpha), \quad p = \rho\omega P(\alpha), \quad \alpha = z\sqrt{\frac{\omega}{\nu}} \quad (2.13)$$

the Eqs (2.8)-(2.11) in term of E , F , G , and P take the following form

$$E' - GE - E^2 + F^2 + 2F - 1 = 0, \quad (2.14)$$

$$F' - GF - 2EF - 2E = 0, \quad (2.15)$$

$$P' - G' + GG = 0, \quad (2.16)$$

$$G + 2E = 0 \quad (2.17)$$

Corresponding boundary condition of Eq (2.12) become

$$\left. \begin{aligned} E(0) = G(0) = 0, F(0) = 1, P(0) - P_0 = 0, \\ E(\infty) = F(\infty) = 0 \end{aligned} \right\} \quad (2.18)$$

Note that G must tend to finite limit, say $-c$, as $\alpha \rightarrow \infty$, i.e., $G(\infty) = -c, (c > 0)$

2.1.2 Parameters of physical interest

Boundary layer displacement thickness

Thickness of boundary layer can be found by calculated the distance over which inertia and viscous forces are comparable. The velocity in the boundary layer attains a value which is very close to the external velocity at a small distance from the wall.

The boundary layer displacement thickness is defined as

$$d = \frac{1}{r\omega} \int_{z=0}^{\infty} v_r dz = \int_{\alpha=0}^{\infty} F(\alpha) d\alpha = 1.3456145 \quad (2.19)$$

Further, total volume flowing outward the z-axis

$$\begin{aligned} Q &= 2\pi R \int_0^{\infty} v_r dz = 2\pi R \int_0^{\infty} r\omega E(\alpha) \sqrt{v} \omega d\alpha \\ &= -\pi R^2 \sqrt{\omega v} G(\infty) = 2.786094 R^2 \sqrt{\omega v} = 2.786094 R^2 v^{\frac{\alpha}{2}} \end{aligned} \quad (2.20)$$

Hence the total volume flowing outward the z-axis is proportional to the dimensionless parameter α

The fluid is taken to rotate at a large distance from the wall, in this case the angle becomes

$$\begin{aligned} \tan \varphi_0 &= - \left(\begin{array}{c} \frac{\partial v_r}{\partial z} \\ \frac{\partial v_\theta}{\partial \theta} \end{array} \right) = - \frac{E(0)}{F(0)} = \frac{0.54}{0.62} = 0.870967 \\ &\Rightarrow \varphi_0 = 41^\circ \end{aligned} \quad (2.21)$$

2.2 Solution of the problem

The value of E, F, G and P are compared graphically with their corresponding value in classical case. Cochran indicated that formal asymptotic expansions (for large α) of the system of Eqs (2.14)-(2.17) are the power series in $\exp(-i\alpha)$, i.e.,

$$E(\alpha) \approx \sum_{i=1}^{\infty} A_i \exp(-i\alpha), \quad (2.22)$$

$$F(\alpha) \approx \sum_{i=1}^{\infty} B_i \exp(-i\alpha), \quad (2.23)$$

$$G(\alpha) \approx G(\infty) + \sum_{i=1}^{\infty} C_i \exp(-i\alpha), \quad (2.24)$$

$$P(\alpha) - P_0 \approx \sum_{i=1}^{\infty} D_i \exp(-i\alpha) \quad (2.24)$$

Integrating the Eqs (2.14) and (2.15) between 0 to ∞ , and using the relations

$$\left. \begin{aligned} \int_0^{\infty} GE \, d\alpha &= [GE]_0^{\infty} - \int_0^{\infty} G E' \, d\alpha = 2 \int_0^{\infty} E^2 \, d\alpha, \\ \int_0^{\infty} GF \, d\alpha &= [GF]_0^{\infty} - \int_0^{\infty} G F' \, d\alpha = 2 \int_0^{\infty} EF \, d\alpha \end{aligned} \right\} \quad (2.25)$$

together with $E(\infty) = 0$ and $F(\infty) = 0$, we get

$$\left. \begin{aligned} -E(0) &= \int_0^{\infty} (3E^2 - F^2 - 2F + 1) \, d\alpha, \\ -F(0) &= \int_0^{\infty} (4EF + 2E) \, d\alpha \end{aligned} \right\} \quad (2.26)$$

Using the supposition $E(0) = a$ and $F(0) = b$ in Eqs (2.14)-(2.18), we get the following additional boundary conditions for the approximate solution

$$\left. \begin{aligned} E'(0) &= -2, & E''(0) &= -4b, \\ F(0) &= 0, & F'(0) &= 4a, \\ G(0) &= 0, & G'(0) &= -2a, & G''(0) &= 4, \\ P(0) &= -2a, & P'(0) &= 8b \end{aligned} \right\} \quad (2.27)$$

First four coefficients in each Eqs (2.22)-(2.24) with the help of Eqs (2.18) and (2.27) are as follow

$$\left. \begin{array}{l}
A_1 + A_2 + A_3 + A_4 = 0 \\
A_1 + 2A_2 + 3A_3 + 4A_4 = \frac{-a}{c} \\
A_1 + 4A_2 + 9A_3 + 16A_4 = -2 \\
A_1 + 8A_2 + 27A_3 + 64A_4 = \frac{4b}{c^3}
\end{array} \right\} \cdot \left. \begin{array}{l}
B_1 + B_2 + B_3 + B_4 = 1 \\
B_1 + 2B_2 + 3B_3 + 4B_4 = \frac{-b}{c} \\
B_1 + 4B_2 + 9B_3 + 16B_4 = 0 \\
B_1 + 8B_2 + 27B_3 + 64B_4 = \frac{-4a}{c^3}
\end{array} \right\} \cdot \left. \begin{array}{l}
-c + C_1 + C_2 + C_3 + C_4 = 0 \\
C_1 + 2C_2 + 3C_3 + 4C_4 = 0 \\
C_1 + 4C_2 + 9C_3 + 16C_4 = \frac{-20}{c^2} \\
C_1 + 8C_2 + 27C_3 + 64C_4 = \frac{-4}{c^3}
\end{array} \right\} \cdot \left. \begin{array}{l}
D_1 + D_2 + D_3 + D_4 = 0 \\
D_1 + 2D_2 + 3D_3 + 4D_4 = \frac{2a}{c} \\
D_1 + 4D_2 + 9D_3 + 16D_4 = \frac{4}{c^3} \\
D_1 + 8D_2 + 27D_3 + 64D_4 = \frac{-8b}{c^3}
\end{array} \right\} \quad (2.28)$$

Solving Eq (2.28), we have

$$\left. \begin{array}{l}
A_1 = \left(-\frac{2b}{3c^3} - \frac{3}{c^2} + \frac{13a}{3c} \right) \quad A_2 = \left(-\frac{2b}{c^3} + \frac{8}{c^2} - \frac{19a}{2c} \right) \\
A_3 = \left(-\frac{2b}{c^3} - \frac{7}{c^2} + \frac{7a}{c} \right) \quad A_4 = \left(\frac{2b}{3c^3} + \frac{2}{c^2} - \frac{11a}{6c} \right) \\
B_1 = \left(\frac{2a}{3c^3} + \frac{13b}{3c} + 4 \right) \quad B_2 = \left(-\frac{2a}{c^3} - \frac{19b}{2c} - 6 \right) \\
B_3 = \left(\frac{2a}{c^3} + \frac{7b}{c} + 4 \right) \quad B_4 = \left(-\frac{2a}{3c^3} - \frac{11b}{6c} - 1 \right)
\end{array} \right\} \quad (2.29)$$

$$\left. \begin{array}{l}
C_1 = \left(\frac{2}{3c^3} - \frac{3a}{c^2} + 4c \right) \quad C_2 = \left(-\frac{2}{c^3} + \frac{8a}{c^2} - 6c \right) \\
C_3 = \left(\frac{2}{c^3} - \frac{7a}{c^2} + 4c \right) \quad C_4 = \left(-\frac{2}{3c^3} + \frac{2a}{c^2} - c \right) \\
D_1 = \left(\frac{4b}{3c^3} + \frac{6}{c^2} - \frac{26a}{3c} \right) \quad D_2 = \left(-\frac{4b}{c^3} - \frac{16}{c^2} + \frac{19a}{c} \right) \\
D_3 = \left(\frac{4b}{c^3} + \frac{14}{c^2} - \frac{14a}{c} \right) \quad D_4 = \left(-\frac{4b}{3c^3} - \frac{4}{c^2} + \frac{11a}{3c} \right)
\end{array} \right\} \quad (2.30)$$

Using the values $a = 0.54$, $b = -0.62$, and $c = 0.866$ [24], one can calculate the numerical values of the coefficient $A_1, A_2, A_3, A_4, B_1, B_2, B_3, B_4, C_1, C_2, C_3, C_4, D_1, D_2, D_3$ and D_4 , as a result the velocity components and asymptotic pressure with the dimensionless parameter α can be obtained easily

2.3 Results and discussion

The problem considered here involves a number of parameters, on the basis of which, a wide range of numerical results have been derived. Of these results, a small section is presented here for brevity. The numerical results for the velocity profiles, commonly known as radial, tangential and axial are shown in Figs (2.2)-(2.4) respectively.

Also, we have calculated the angle between the wall and revolving ferrofluid which is 41° . In Fig (2.2), the curve E_2 represent the effect of rotation on radial velocity in case of ferrofluid flow due to rotating disk, whereas E_1 indicates the radial velocity profile of the Cochran's study of ordinary viscous fluid flow. Due to rotation the radial velocity reaches its maximum value near the surface of the disk with magnitude 0.08894 at $\alpha = 0.4$, whereas, in Cochran case, the maximum value 0.181 of radial velocity is attained comparatively at distant point $\alpha = 0.9$. Here, it is noticed that the radial velocity E_2 has very less peak value in comparison to E_1 because of thickening of the fluid layer due to the rotation of the whole system. Thus, the effect of rotation is more pronounced than the force of magnetization in the sense of fluid thickening. Also it is quite interesting to see that in case of rotation before converging to zero, the radial velocity once become negative.

Fig (2.3) is the graphical comparison of the tangential velocity of ferrofluid flow with rotation F_2 to that of Cochran's ordinary viscous fluid F_1 . In our case, we increase the value of α the tangential velocity F_2 decreases continuously and tends to zero for large value of α . It is observed from the table (2.1), the value of tangential velocity is 0.49762 at $\alpha = 1$, whereas for the ordinary viscous fluid, the tangential velocity is 0.46800 for the same value of α . Therefore at $\alpha = 1$, there is an approximate increment of 6.7% in the value of tangential velocity in comparison to that of Cochran value. From the figures, It is clear that F_1 converges to zero little faster than F_2 however, both the curves have similar trends.

Fig (2.4) show that axial velocity profile, which is zero in the beginning and tends to finite value -0.886 for $\alpha = 14.8$ onwards. When we increase the value of α , it decreases continuously in the negative region. Our axial velocity value is -0.23858 at $\alpha = 1$, whereas for Cochran, the axial velocity is -0.266 for the same value of α .

Meaning thereby, for the same value of α the axial velocity component acquires large value then the value in ordinary case

The pressure profile $P(\alpha) - P_0$ with the initial pressure P_0 at $\alpha = 0$ is shown in Fig (2.5). Here pressure goes to negative region near the surface of the disk, and at $\alpha = 0.4$ it goes to maximum negative value -0.17909 . Onwards to $\alpha = 0.4$, pressure starts increasing with increasing the value of α and $\alpha = 1.3$, it enters in the positive region and attains maximum value 0.07667 at $\alpha = 2.2$. Finally $P(\alpha) - P_0$ converges to zero i.e., $P(\alpha)$ converges to P_0 .

Comparing Fig (2.3) and Fig (2.5), we conclude that when radial velocity increases, the pressure of the ferrofluid decreases and when radial velocity decreases, ferrofluid pressure increases i.e., they are converse in convergence behavior. Also, tangential velocity diminishes slower than axial velocity component. The change in the curve of radial velocity is faster due to effect of external magnetic field resulting in reducing the time required for velocity profile to reach there convergence level. In Fig (2.6) and Fig (2.7), derivatives of radial and tangential components of velocities are shown.

In nut shell, the rotation of the disk along with revolution of the ferrofluid results in an increased displacement thickness 1.34562 more than that of [25].

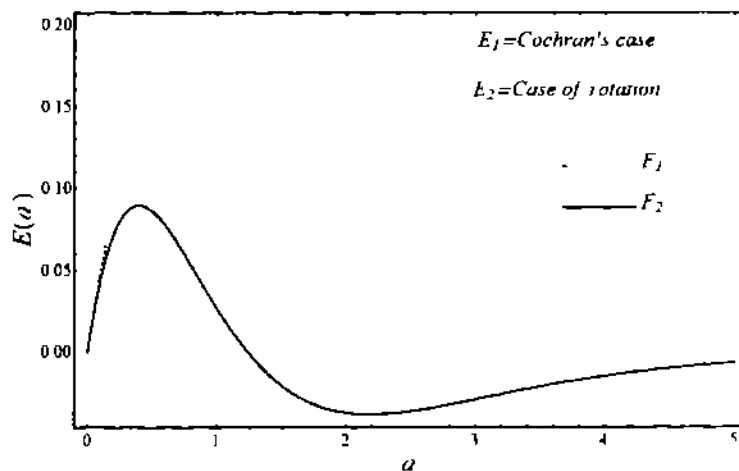


Fig. 2.2: Effect of rotation on radial velocity profile

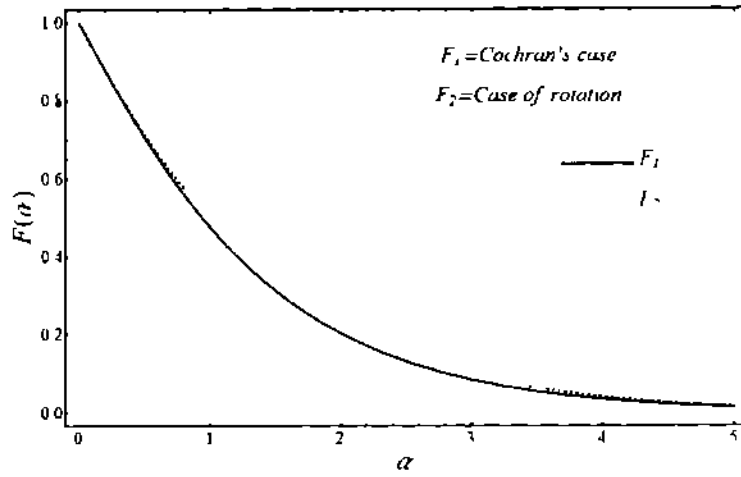


Fig. 2.3: Effect of rotation on tangential velocity profile

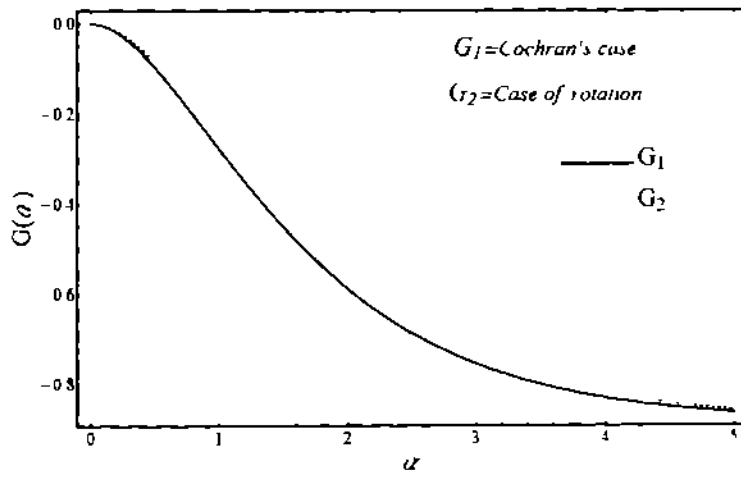


Fig. 2.4: Effect of rotation on axial velocity profile

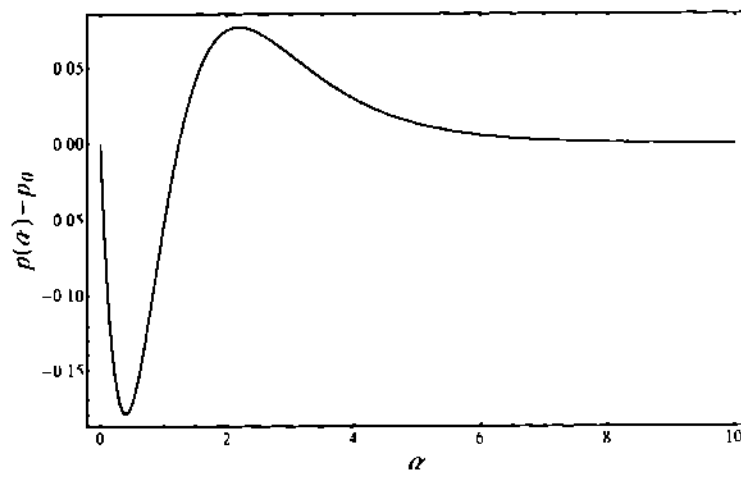


Fig. 2.5: Effect of rotation on pressure profile

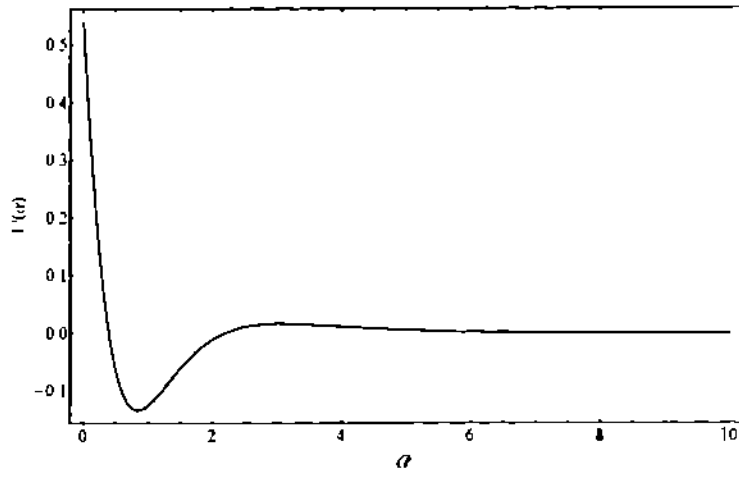


Fig. 2.6: Derivative of radial velocity

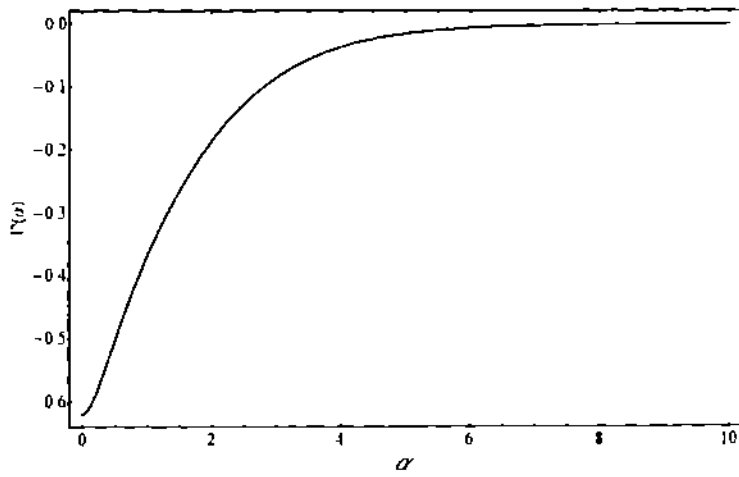


Fig. 2.7: Derivative of tangential velocity

The present numerical results are presented in table (2.1) that give very good approximate solution of the above system of non-linear differential equations

Table 2.1: The study state velocity field and pressure as a function of α

α	E	F	G	$P(\alpha) - P_0$	E	F
0	0	1	0	0	0.54	-0.6200
0.4	0.08894	0.765722	-0.05778	-0.17909	-0.0046	-0.53308
0.8	0.0528076	0.576094	-0.17309	-0.10562	-0.1332	-0.41783
1.2	0.0035476	0.4286140	-0.30498	-0.00710	-0.10210	-0.32301
1.6	-0.0262658	0.3152410	-0.43171	0.05253	-0.04825	-0.24658
2.0	-0.0373981	0.229349	-0.54162	0.074796	-0.01078	-0.18521
4.0	-0.0148249	0.04218	-0.81773	0.029650	0.01132	-0.03673
6.0	-0.0028179	0.00727434	-0.87408	0.005635	0.00244	-0.00643
8.0	-0.0006941	0.00124	-0.88397	0.000976	0.00043	-0.00110
12.0	-0.00001415	0.0000358	-0.88594	0.000028	1.3E-05	-3.2E-05
∞	0	0	-0.886	0	0	0

2.4 Concluding remarks

From these result we conclude that magnetization force *i.e.*, $\mu_0(M \nabla)H$ reduce the pressure. Also, it has been observed that magnetic field intensity increases the radial velocity, whereas, the fluid rotation has reverse effect. The effect of rotation is more pronounced than the force of magnetization due to which the radial velocity takes very less peak value in comparison to ordinary viscous fluid flow case. Due to the rotation, the retardation of radial velocity increase the thickness of the magnetic field layer.

Chapter 3

On the boundary layer flow of ferrofluids

The purpose of the present problem is to theoretically examine the magneto-viscous effects on axisymmetric unsteady flow of an incompressible non-conducting nano-Ferrofluid on a rotating disk under the influence of low oscillating magnetic field. The problem has been formulated by employing the basic idea of the Shliomis theory to the equation of motion and magnetization equation for nano-Ferrofluid flow due to a rotating disk. The system of nonlinear partial differential equations governing the unsteady flow is expressed in cylindrical coordinates taking z-axis as axis of rotation and are further solved with homotopy analysis method (HAM) based Bvph 2.0 package by taking the initial guess and linear operator. The nature of velocity profile and temperature distribution in the presence of low oscillating magnetic field with different values of particle concentration and effective magnetization parameters are discussed graphically. The physical parameters like shear stress at wall, heat transfer rate through wall, boundary layer thickness and volume flow rate in axial direction are presented by tabular form.

3.1 Formulation of the problem

3.1.1 Flow modelling

Consider the axially symmetric laminar and non-conducting flow of an incompressible nano-Ferrofluid past a stretchable rotating disk. The disk has stretching speed $\Omega, r/1-\beta t$ which is proportional to the radius r and has an angular velocity $\alpha \Omega, r/1-\beta t$ varying with time. The coordinate system and geometry of the problem are shown in Fig. 3.1.

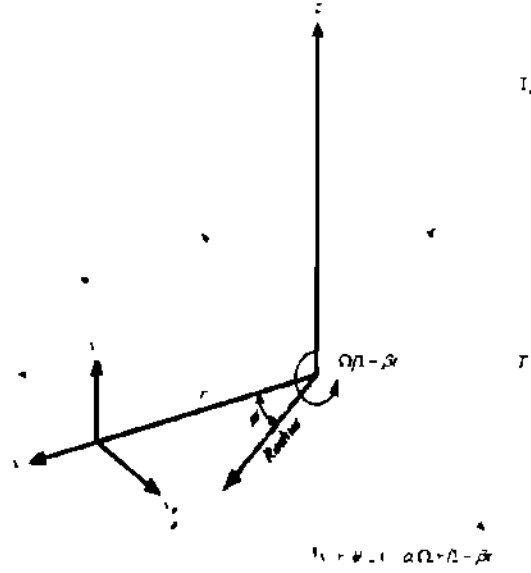


Fig. 3.1: Geometry of the problem

The system of Ferro-hydrodynamic governing equations consisting of equation of continuity, equation of motion, temperature equation, magnetization equation and equation of rotational motion in vector form are

$$\nabla \cdot \mathbf{V} = 0, \quad (3.1)$$

$$\rho_{nf} \frac{d\mathbf{V}}{dt} = -\nabla p + \mu_{nf} \nabla^2 \mathbf{V} + \mu_0 (\mathbf{M} \cdot \nabla) \mathbf{H} + \frac{1}{2\tau_1} \nabla \times (\omega_p - \Omega), \quad (3.2)$$

$$(\rho C_p)_{nf} \frac{dT}{dt} = k_{nf} \nabla^2 T, \quad (3.3)$$

$$\frac{d\mathbf{M}}{dt} = \omega_p \times \mathbf{M} - \frac{1}{\tau_B} (\mathbf{M} - \mathbf{M}_0), \quad (3.4)$$

$$\mathbf{I} \frac{d\omega_p}{dt} = \mathbf{M} \times \mathbf{H} - \frac{1}{\tau_1} (\omega_p - \Omega) \quad (3.5)$$

In above, $\mathbf{V} = (v_x, v_y, v_z)$ is velocity, T is temperature, \mathbf{M} is magnetization of the fluid, \mathbf{H} is strength magnetic field, τ_1 is Relaxation time parameter, τ_B is Brownian relaxation time, μ_0 is permeability of free space, \mathbf{I} is sum of moments of inertia of the particles per unit volume, ω_p is internal angular momentum due to the self-rotation of particles and Ω is the vorticity of the flow. The complete set of equations also includes the Maxwell's equations

$$\nabla \times \mathbf{H} = 0, \nabla \cdot (\mathbf{H} + 4\pi \mathbf{M}) = 0 \quad (3.6)$$

The magnetization of the fluid M with the relation of strength magnetic field H is given as

$$M = M_s \left(\coth \xi - \frac{1}{\xi} \right), \quad (3.7)$$

where $M_s = \Phi M_0$ is the saturation magnetization of the liquid, being determined by the volume concentration of the magnetic component Φ and its instantaneous magnetization M_0 [26-28]. At $\tau_B = 0$, the instantaneous equilibrium magnetization M_0 is given as

$$M_0 = nmL(\xi) \frac{H}{H}, \quad \xi = \frac{mH}{kT}, \quad L(\xi) = \text{Coth } \xi - \xi^{-1}, \quad (3.8)$$

where n is the number of particle, m is the magnetic moment of the particle, $L(\xi)$ is the Langevin function, ξ is the Langevin parameter (ratio of magnetization energy to the thermal energy) and k is the Boltzmann constant. Since, τ_i is small, the inertial term is negligible in comparison with relaxation term i.e., $I \frac{d\omega_p}{dt} \ll I \frac{\omega_p}{\tau_i}$, therefore,

Eq (3.5) can be written as

$$\omega_p = \Omega + \frac{\tau_i}{I} (M \times H) \quad (3.9)$$

Now, Eqs (3.2) and (3.4) in view of Eq (3.9) can be written as

$$\rho_m \frac{dV}{dt} = -\nabla p + (M \cdot \nabla) H + \mu_m \nabla^2 V + \frac{1}{2} \nabla \times (M \times H), \quad (3.10)$$

$$\frac{dM}{dt} = \Omega \times M - \frac{1}{\tau_B} (M - M_0) + \frac{\tau_i}{I} M \times (M \times H) \quad (3.11)$$

Magnetic torque and viscous torque are acting on the particles denoted by $M \times H$ and $(\omega_p - \Omega)$ respectively. The equilibrium of both torques, leads to the interference of the particle rotation, can be written as

$$M \times H = -6\mu_m \phi (\Omega - \omega_p), \quad (3.12)$$

and at equilibrium

$$M = \frac{\phi M_s L(\xi_c) \xi_c}{\xi} \quad (3.13)$$

Where ϕ is the volume fraction and ξ_e denotes the effective magnetic field parameter (the ratio of effective magnetic force to the thermal force i.e., $\xi_e = \frac{mH_e}{kT}$)

In the presence of slow oscillating magnetic field Eq (3 11) can be written as [29-33]

$$\frac{d}{dt} \left(L_e \frac{\xi_e}{\xi} \right) = \Omega \times \left(L_e \frac{\xi_e}{\xi} \right) - \frac{1}{\tau_B} \frac{L_e}{\xi_e} (\xi_e - \xi) - \frac{L_e^2}{2\tau_B \xi_e} \xi_e \times (\xi_e - \xi) \quad (3 14)$$

The effective field can be expressed by the equation of zero approximation from the Eq (3 14) as

$$\tau_B \frac{d\xi_e}{dt} = - \left(\frac{d \log L_e}{d \xi_e} \right)^{-1} \left(1 - \frac{\xi_e}{\xi_0} \cos \omega_0 t \right) \quad (3 15)$$

Here, the parameter ξ_0 is the amplitude of the real magnetic field, L_e is the effective Langevin function, ω_0 is the frequency of the field. From [34], using linear approximations in $\Omega \tau_B$ and the expression

$$\mathbf{M}^{(1)} = \mathbf{M}^{(0)} R(\xi_e) \tau_B \Omega \times \mathbf{h}, \quad (3 16)$$

where $\mathbf{M}^{(0)} = \phi \mathbf{M}_s L(\xi)$ and \mathbf{h} is unit vector along the applied field, Eq (3 14) reduces to

$$\tau_B \frac{dR(\xi_e)}{dt} = \left(1 - \frac{1}{2} \left(\frac{1}{L_e} - \frac{1}{\xi_e} \right) \xi_0 R(\xi_e) \cos \omega_0 t \right) \quad (3 17)$$

Since magnetic torque is not equal to zero, so from Eqs (3 12) and (3 17), the expression for mean magnetic torque becomes

$$\overline{\mathbf{M} \times \mathbf{H}} = -6\mu\phi\Omega g, \quad g = \frac{1}{2} \xi_0 \overline{\cos \omega_0 t L(\xi_e) R(\xi_e)} \quad (3 18)$$

Here, $g(\xi_0, \omega_0 \tau_B)$ is the effective magnetization parameter, if $\omega_0 \tau_B < 1$ (in the low oscillating field) the Magnetic fluid viscosity under and alternating magnetic field become larger than the Magnetic fluid viscosity in zero field

$$\begin{aligned} \frac{1}{2} \nabla \times \overline{\mathbf{M} \times \mathbf{H}} &= \frac{1}{2} \nabla \times -6\mu_{nf} \phi g \Omega = -\frac{3}{2} \mu_{nf} \phi g \nabla (\nabla \cdot \mathbf{V}) + \frac{3}{2} \mu_{nf} \phi g \nabla^2 \mathbf{V} \\ &= \frac{3}{2} \mu_{nf} \phi g \nabla^2 \mathbf{V} \end{aligned} \quad (3 19)$$

Now the Eq (3 10) with the help of Eq (3 19) can be written as

$$\rho_{nf} \frac{d\mathbf{V}}{dt} = -\nabla p + (\mathbf{M} \cdot \nabla) \mathbf{H} + \mu_{nf} \left(1 + \frac{3}{2} \phi g \right) \nabla^2 \mathbf{V}, \quad (3 20)$$

$$\rho \frac{dV}{dt} = -\nabla \tilde{p} + \left(1 + \frac{3}{2} \phi g\right) \mu_{nf} \nabla^2 V \quad (3.21)$$

As $-\nabla \tilde{p} = -\nabla p + (M \nabla) H$ i.e., is reduced pressure. In the investigation, unsteady, axially-symmetric, incompressible flow of an electrically non-conducting fluid has been considered, assuming that the viscosity is dependent on the magnetic field and thermal effects are not taken under consideration. The disk rotates about z -axis with constant angular velocity ω , where z is the vertical z -axis in the cylindrical coordinate system with r and θ are the radial and tangential axis respectively, and the flow is considered axis-symmetric and incompressible, so the equation of motion and continuity can be written in the cylindrical form as [35,36]

$$\frac{\partial v_r}{\partial r} + \frac{v_r}{r} + \frac{\partial v_z}{\partial z} = 0, \quad (3.22)$$

$$\begin{aligned} -\frac{\partial \tilde{p}}{\partial r} + \mu_{nf} \left(1 + \frac{3}{2} \phi g\right) \left[\frac{\partial^2 v_r}{\partial r^2} + \frac{\partial}{\partial r} \left(\frac{v_r}{r} \right) + \frac{\partial^2 v_r}{\partial z^2} \right] \\ = \rho_{nf} \left[\frac{\partial v_r}{\partial t} + v_r \frac{\partial v_r}{\partial r} + v_z \frac{\partial v_r}{\partial z} - \frac{v_r^2}{r} \right], \end{aligned} \quad (3.23)$$

$$\begin{aligned} \mu_{nf} \left(1 + \frac{3}{2} \phi g\right) \left[\frac{\partial^2 v_\theta}{\partial r^2} + \frac{\partial}{\partial r} \left(\frac{v_\theta}{r} \right) + \frac{\partial^2 v_\theta}{\partial z^2} \right] \\ = \rho_{nf} \left[\frac{\partial v_\theta}{\partial t} + v_r \frac{\partial v_\theta}{\partial r} + v_z \frac{\partial v_\theta}{\partial z} + \frac{v_r v_\theta}{r} \right]. \end{aligned} \quad (3.24)$$

$$\begin{aligned} -\frac{\partial \tilde{p}}{\partial z} + \mu_{nf} \left(1 + \frac{3}{2} \phi g\right) \left[\frac{\partial^2 v_z}{\partial r^2} + \frac{1}{r} \frac{\partial v_z}{\partial r} + \frac{\partial^2 v_z}{\partial z^2} \right] \\ = \rho_{nf} \left[\frac{\partial v_z}{\partial t} + v_r \frac{\partial v_z}{\partial r} + v_z \frac{\partial v_z}{\partial z} \right], \end{aligned} \quad (3.25)$$

$$(\rho C_p)_{nf} \left[\frac{\partial T}{\partial t} + v_r \frac{\partial T}{\partial r} + v_z \frac{\partial T}{\partial z} \right] = k_{nf} \left[\frac{\partial^2 T}{\partial r^2} + \frac{1}{r} \frac{\partial T}{\partial r} + \frac{\partial^2 T}{\partial z^2} \right], \quad (3.26)$$

along the following boundaries conditions

$$\left. \begin{aligned} \text{at } z=0, \quad v_r = \frac{\alpha \Omega r}{1 - \beta t}, \quad v_\theta = \frac{\Omega r}{1 - \beta t}, \quad v_z = 0, \quad T(r, \theta, z) = T_w \\ \text{at } z = \infty, \quad v_r = 0, \quad v_\theta = 0, \quad T(r, \theta, z) = T_\infty \end{aligned} \right\} \quad (3.27)$$

Now, introduce the following similarity transformation

$$\left. \begin{aligned} \eta &= \sqrt{\frac{\Omega}{\nu_f}} \frac{z}{\sqrt{1-\beta t}}, \quad v_r(r, \theta, z) = \frac{\Omega r}{1-\beta t} F(\eta), \quad v_\theta(r, \theta, z) = \frac{\Omega r}{1-\beta t} G(\eta), \\ v_z(r, \theta, z) &= \sqrt{\frac{\Omega \nu_f}{1-\beta t}} E(\eta), \quad \theta(\eta) = \frac{T - T_\infty}{T_w - T_\infty}, \quad \frac{p}{\rho_f} = -\frac{\Omega \nu_f}{1-\beta t} P(\eta) \end{aligned} \right\} \quad (3.28)$$

By using Eq (3.28) into Eq (3.22) to (3.26) and get the system of nonlinear ordinary differential equations in dimensionless form as

$$2F(\eta) + E'(\eta) = 0, \quad (3.29)$$

$$\frac{\rho_{nf}}{\rho_f} \left[F^2 - G^2 + EF' + S \left(F + \frac{\eta}{2} F' \right) \right] = \frac{\mu_{nf}}{\mu_f} \left(1 + \frac{3}{2} \phi g \right) F'', \quad (3.30)$$

$$\frac{\rho_{nf}}{\rho_f} \left[EG' + 2FG + S \left(G + \frac{\eta}{2} G' \right) \right] = \frac{\mu_{nf}}{\mu_f} \left(1 + \frac{3}{2} \phi g \right) G'', \quad (3.31)$$

$$\frac{\rho_{nf}}{\rho_f} \left[EE' + \frac{S}{2} (E + \eta E') \right] = -\frac{\partial P}{\partial \eta} + \frac{\mu_{nf}}{\mu_f} \left(1 + \frac{3}{2} \phi g \right) E'', \quad (3.32)$$

$$\frac{(\rho C_p)_{nf}}{(\rho C_p)_f} \text{Pr} \left[E\theta' + S \frac{\eta}{2} \theta' \right] = \frac{k_{nf}}{k_f} \theta'', \quad (3.33)$$

and corresponding boundary condition are

$$\left. \begin{aligned} F(0) &= \alpha, \quad G(0) = 1, \quad E(0) = 0, \quad \theta(0) = 1, \\ F(\infty) &= 0, \quad G(\infty) = 0, \quad \theta(\infty) = 0 \end{aligned} \right\} \quad (3.34)$$

Where, $\text{Pr} = \frac{\mu_f C_{pf}}{k_f}$ is modified Prandtl number and $S = \frac{\beta}{\Omega}$ is the unsteadiness

parameter

3.1.2 Thermodynamics properties

In the Eqs (3.22) to (3.26), the effective density is ρ_{nf} , heat capacitance is $(C_p)_{nf}$,

viscosity is μ_{nf} , and thermal conductive k_{nf} of the nano-ferrofluid defined as

$$\rho_{nf} = (1 - \phi_s) \rho_f + \phi_s \rho_s, \quad (3.35)$$

$$(\rho C_p)_{nf} = (1 - \phi_s) (\rho C_p)_f + \phi_s (\rho C_p)_s, \quad (3.36)$$

$$k_{nf} = \frac{k_s + 2k_f + 2\phi_s (k_s - k_f)}{k_s + 2k_f - \phi_s (k_s - k_f)} k_f, \quad (3.37)$$

$$\mu_{nf} = \mu_f \left(1 - \frac{\phi_s}{\phi_{\max}} \right)^{-2.5 \phi_{\max}} \quad (3.38)$$

Here, ϕ_a is the solid volume fraction of a particles aggregate, ρ_f , ρ_a , $(C_p)_f$ and $(C_p)_a$ are the densities and heat capacitances of base fluid and aggregate respectively The μ_f is viscosity of the base fluid, k_f and k_a are thermal conductivities of base fluid and particle aggregation respectively The thermal properties of particle aggregation are defined as

$$\rho_a = (1 - \phi_{in})\rho_f + \phi_{in}\rho_s, \quad (3.39)$$

$$(C_p)_a = (1 - \phi_{in})(C_p)_f + \phi_{in}(C_p)_s, \quad (3.40)$$

Above $(C_p)_s$ is heat capacitance of the particle, and ϕ_{in} is the volume fraction of the nanoparticles in the aggregate or the cluster The thermal conductivities of aggregates are estimated by separating them into two components, the percolation contributing backbone, and non-percolation contributing dead-end particles Considering the interfacial thermal resistance (Kapitza resistance), the effective thermal conductivity of dead-end particles based suspension (including the basefluid and dead-end particles) is given by using Bruggeman model

$$(1 - \phi_{nc})(k_f - k_{nc}) / (k_f + 2k_{nc}) + \phi_{nc}(k_s - k_{nc}) / (k_s + 2k_{nc}) = 0 \quad (3.41)$$

The effective thermal conductivity of aggregate, k_a is determined by using composite theory for misoriented ellipsoidal particles for the backbone, in a matrix of non-percolation contributing portion, the following equations are used

$$k_a = k_{nc} \frac{3 + \phi_c [2\beta_{11}(1 - L_{11}) + \beta_{33}(1 - L_{33})]}{3 - \phi_c [2\beta_{11}L_{11} + \beta_{33}L_{31}]}, \quad (3.42)$$

where

$$\left. \begin{aligned} L_{11} &= 0.5p^2 / (p^2 - 1) - 0.5p \cosh^{-1} p / (p^2 - 1)^{1.5}, \\ L_{33} &= 1 - 2L_{11}, \\ \beta_{ii} &= (k_{ii}^c - k_{nc}) / [k_{nc} - L_{ii}(k_{ii}^c - k_{nc})] \end{aligned} \right\} \quad (3.43)$$

Interfacial resistance is accounted for in the term

$$k_{ii}^c = k_s / (1 + \gamma L_{ii} k_s / k_f) \quad (3.44)$$

Here $\gamma = (2 + 1/p)\alpha$, $\alpha = A_k / a_i$ and A_k is the Kapitza radius In Eq (3.44) p is aspect ratio, for which the cluster spanning chain is given by $p = R_k / a_i$ In particular, our treatment allows the effect of cluster morphology to be evaluated in terms of the

average radius of gyration R_g , the fractal dimensions d_f and chemical dimension d_c of the aggregates, respectively. Following the definition of the fractal dimension d_f , the number of particles in aggregation is given by

$$N_{mt} = \left(\frac{R_g}{a_1} \right)^{d_f}, \quad (3.45)$$

Where a_1 is the radius of the primary particle. Due to number conservation of the nanoparticles, $\phi = \phi_{mt} \phi_n$, where ϕ is the volume fraction of the nanoparticles. It can be shown that $\phi_{mt} = \left(\frac{R_g}{a_1} \right)^{1-d_f}$ and $\left(\frac{R_g}{a_1} \right)_{max} = \phi^{1/d_f}$ for which $\phi_n = 1$. The number of particles in belonging to backbone N_c is the chemical dimension is given by

$$N_c = \left(\frac{R_g}{a_1} \right)^{d_c}, \quad (3.46)$$

Where d_c ranges between one and d_f . When $d_c = d_f$, all of the particles belong to the backbone, and there are no dead ends. Therefore, the volume fraction of backbone particles ϕ_c in the aggregate is given by $\phi_c = \left(\frac{R_g}{a_1} \right)^{d_c}$. The volume fraction of the particles belonging to dead ends ϕ_n is given by

$$\phi_n = \phi_{mt} - \phi_c \quad (3.47)$$

3.1.3 Parameters of physical interest

Skin friction coefficient and Nusselt number

The skin friction coefficient C_f and the Nusselt number Nu are physical quantities which are given by

$$C_f = \frac{\sqrt{\tau_{ur}^2 + \tau_{u\phi}^2}}{\rho_f \left(\frac{\alpha \Omega r}{1 - \beta t} \right)^2}, \quad Nu = \frac{r q_w}{k_f (T_w - T_\infty)} \quad (3.48)$$

Where τ_{ur} and $\tau_{u\phi}$ are the radial and the transversal skin friction or shear stress at the surface of disk, respectively, and q_w is the surface heat flux, introduced as

$$\tau_{ur} = \mu_{nf} \left(1 + \frac{3}{2} \phi g \right) \left(\frac{\partial v_r}{\partial z} + \frac{\partial v_z}{\partial \theta} \right)_{z=0}, \quad \tau_{u\phi} = \mu_{nf} \left(1 + \frac{3}{2} \phi g \right) \left(\frac{\partial v_\theta}{\partial z} + \frac{1}{r} \frac{\partial v_z}{\partial \theta} \right)_{z=0}, \quad (3.49)$$

$$q_w = -k_{nf} (T_z)_{z=0}$$

Substituting Eqs (3 28) and (3 38) in Eq (3 49) and using Eq (3 48), we have

$$\text{Re}^{\frac{1}{2}} C_f = \frac{\sqrt{F'(0)^2 + G'(0)^2}}{(1-\phi)^{2.5}}, \quad \text{Re}^{-\frac{1}{2}} Nu = -\frac{k_m}{k_f} \theta'(0) \quad (3 50)$$

Here $\text{Re} = \Omega r^2 v_f (1-\beta t)$ is the rotational Reynolds number

Boundary layer displacement thickness

Thickness of boundary layer can be found by finding the separation over inertia and viscous forces are practically identical. The velocity in the boundary layer accomplishes a value which is near the external velocity as of now at a little separation from the wall. The boundary layer displacement thickness is ascertained as

$$d = \frac{1-\beta t}{\Omega r} \int_{z=0}^{\infty} v_\theta dz = r \text{Re}^{-\frac{1}{2}} \int_{\eta=0}^{\infty} G(\eta) d\eta \quad (3 51)$$

Total volume flowing outward the z-axis,

$$Q = 2\pi r \int_0^{\infty} v_r dz = 2\pi r v_f \text{Re}^{\frac{1}{2}} \int_0^{\infty} F(\eta) d\eta \quad (3 52)$$

The fluid is taken to rotate at a large distance from the wall, the angle becomes

$$\tan(\psi_0) = - \left(\begin{array}{c} \frac{\partial v_r}{\partial v_\theta} \\ \frac{\partial v_\theta}{\partial v_z} \end{array} \right) = - \frac{F'(\eta)}{G'(\eta)} = -10.67 = -84.6^\circ \quad (3 53)$$

3.2 Solution of the problem

Due to nonlinear nature of Eqs (3 29)-(3 33), an exact solution is not possible. Now, we opted to go for analytic solution. To this end, the Mathematica package BVPh 2.0 which is based on the homotopy analysis method employed for solving nonlinear ordinary differential equation using computational software Mathematica 9. For simplicity, the BVPh 2.0 needs to input the governing equations along with corresponding boundary conditions and choose proper initial guess of solutions and auxiliary linear operators for under consideration linear sub-problems. In this package, one has great freedom to choose the auxiliary linear operator and initial guess, thus we choose the auxiliary linear operators and initial guess for the desired solutions as follow

TH-16774

$$\left. \begin{aligned} \mathcal{L}_E(H) &= \frac{dE}{d\eta}, \quad \mathcal{L}_F(F) = \frac{dF}{d\eta} + \frac{d^2F}{d\eta^2}, \\ \mathcal{L}_G(G) &= \frac{dG}{d\eta} + \frac{d^2G}{d\eta^2}, \quad \mathcal{L}_\theta(\theta) = 2\frac{d\theta}{d\eta} + \frac{d^2\theta}{d\eta^2}, \end{aligned} \right\} \quad (354)$$

$$\left. \begin{aligned} E_o &= 0, \quad F_o(\eta) = \alpha e^{-\eta}, \\ G_o(\eta) &= e^{-\eta}, \quad \theta_o(\eta) = e^{-2\eta} \end{aligned} \right\} \quad (355)$$

so far, we have defined all the input of this problem properly, except the convergence-control parameters. Usually, the optimal values of the convergence-control parameters are obtained by minimizing the squared residual error as follow

$$E_H = \int_0^\infty (2F(\eta) + H'(\eta))^2 d\eta, \quad (356)$$

$$E_F = \int_0^\infty \left(\frac{\rho_{nf}}{\rho_f} \left[F^2 - G^2 + HF' + S \left(F + \frac{\eta}{2} F' \right) \right] - \frac{\mu_{nf}}{\mu_f} \left(1 + \frac{3}{2} \phi g \right) F'' \right)^2 d\eta \quad (357)$$

$$E_G = \int_0^\infty \left(\frac{\rho_{nf}}{\rho_f} \left[HG' + 2FG + S \left(G + \frac{\eta}{2} G' \right) \right] - \frac{\mu_{nf}}{\mu_f} \left(1 + \frac{3}{2} \phi g \right) G'' \right)^2 d\eta. \quad (358)$$

$$E_\theta = \int_0^\infty \left(\frac{(\rho C_p)_{nf}}{(\rho C_p)_f} \text{Pr} \left[H\theta' + S \frac{\eta}{2} \theta' \right] - \frac{k_{nf}}{k_f} \theta'' \right)^2 d\eta \quad (359)$$

In addition to this, the convergence of homotopy series can be accelerated by using either the iteration approach or by applying the homotopy-pade approximations. Both of these techniques can also be employed to obtain the problem solution by directly using some simple commands. Further, the results for velocity components and temperature up to first iteration are as follow

$$\begin{aligned} F = & \left(\frac{1}{2} + \frac{83}{400} \left(\frac{\mu_{nf}}{\mu_f} \right) + \frac{83}{800} \left(\frac{\rho_{nf}}{\rho_f} \right) - \right. \\ & \left. \frac{83S}{1600} \left(\frac{\rho_{nf}}{\rho_f} \right) - \frac{249}{800} \left(\frac{\mu_{nf}}{\mu_f} \right) g\phi \right) e^{-z} \\ & + \left(\frac{-83}{400} \left(\frac{\mu_{nf}}{\mu_f} \right) + \frac{83S}{1600} \left(\frac{\rho_{nf}}{\rho_f} \right) - \right. \\ & \left. \frac{83S}{800} \left(\frac{\rho_{nf}}{\rho_f} \right) z - \frac{249}{800} \left(\frac{\mu_{nf}}{\mu_f} \right) g\phi \right) e^{-2z} - \left(\frac{83}{800} \left(\frac{\rho_{nf}}{\rho_f} \right) \right) e^{-3z}. \end{aligned} \quad (360)$$

$$G = \left(1 + \frac{43}{200} \left(\frac{\mu_{nf}}{\mu_f} \right) - \frac{43}{600} \left(\frac{\rho_{nf}}{\rho_f} \right) - \frac{43S}{800} \left(\frac{\rho_{nf}}{\rho_f} \right) + \frac{192}{400} \left(\frac{\mu_{nf}}{\mu_f} \right) g\phi \right) e^{-z} + \left(-\frac{43}{200} \left(\frac{\mu_{nf}}{\mu_f} \right) + \frac{43S}{800} \left(\frac{\rho_{nf}}{\rho_f} \right) - \frac{43S}{400} \left(\frac{\rho_{nf}}{\rho_f} \right) z - \frac{192}{400} \left(\frac{\mu_{nf}}{\mu_f} \right) g\phi \right) e^{-2z} - \left(\frac{43}{600} \left(\frac{\rho_{nf}}{\rho_f} \right) \right) e^{-3z}, \quad (3.61)$$

$$E = e^{-2z} \left(-\frac{73}{100} + \frac{73}{100} \right), \quad (3.62)$$

$$T = \left(-\frac{53}{75} \left(\frac{k_{nf}}{k_f} \right) - \frac{53}{225} \text{Pr} S - \frac{53}{300} \text{Pr} S \left(\frac{(\rho C_p)_{nf}}{(\rho C_p)_f} \right) z \right) e^{-3z} + \left(1 + \frac{53}{75} \left(\frac{k_{nf}}{k_f} \right) + \frac{53}{225} \text{Pr} S \left(\frac{(\rho C_p)_{nf}}{(\rho C_p)_f} \right) \right) e^{-2z}, \quad (3.63)$$

3.3 Results and discussion

In this chapter, the behavior of emerging parameters involved in the expression of velocity and temperature distributions are examined through Figs (3.2)-(3.9) with water based nano-ferrofluid contained Iron nanoparticles in water. In this study, low isolating magnetic field effect is taken to account. For preparing these figures, consider the radius of gyration is 200 nm there as each sphere shape particles has 10nm radius. In single aggregation, the total particles are 200 in which 50 particles belong to backbone. Figs (3.2)-(3.4) represent radial, tangential and axial velocity profiles for different value of particle concentration against a dimensionless parameter η . In these Figs, it is noticed that several velocity lines have been publicized corresponding to different concentration of nanoparticles. By diverse concentration, unlike collisions between neighboring particles in a fluid are produced different velocity lines. It is also noticed that when the nanoparticle concentration is enhanced the all velocity components are declined. This is accordance with the physical expectation because heighten of resistance between adjacent layers of moving fluid, the base fluid has much velocity as compared to nanofluid. Fig (3.5) shows the effect of particle concentrations on temperature profile. It is seen that the temperature of

nanofluid is enhanced by cumulative of nanoparticles volume fraction. When the nanoparticle volume fraction increases, thermal conduction of the fluid increases that make a cause of enhancement in temperature.

Figs (3.6)-(3.8) characterize the radial, tangential and axial velocities profiles for various value of effective magnetization parameters. It is observed that when the effective magnetization parameter is boosted, the all velocity components are increased. When magnetization parameter is decreased, the angular velocity of the particle increased. In addition, the free rotation of the particle in the flow is damped and increases the fluid flow resistance, consequently result in increased velocity. Fig (3.9) shows the effect of magnetization parameter on temperature profile. In this Fig it is seen that the temperature is amplified with in boosted influence of magnetization parameter.

The numerical sets of values show the results for parameters of physical interest. The impact of particle volume fraction on skin-friction coefficient, local Nusselt, boundary layer thickness and volume flowing outward the z -axis are shown in table (3.1). Skin friction arises when a fluid flows over a solid surface. The fluid is in contact with the surface of the body, resulting in a friction force exerted on the surface. It is seen that when nanoparticle volume fraction enhances shear stress at wall is increased. The shear stress depends on the dynamic viscosity and the gradient of the velocity. It is found that when particle concentration is increased, the gradient of the velocity and dynamic viscosity increases that are caused in enhancement in shear stress at wall. In table (3.1), it is observed that when nanoparticle volume fraction enhances, heat transfer rate at wall increases. Thermal conductivity of fluid plays an important role in the heat transfer rate. For example, enhancement in thermal conductivity of fluid is found 25.13% and 54.85% at 5% and 10% concentration of nanoparticles. Then with same trend, enhancement in heat transfer rate at wall is found 22.39% and 46.93% at 5% and 10% concentrations. With the increasing effect of concentration, total volume flowing outward the z -axis is decreased. Boundary layer thickness is frequently used boundary layer property describes the difference between the case with hypothetical flow over a surface without a boundary layer and the actual flow with a boundary layer. It is noticed that boundary layer thickness decreases corresponding to concentration of particle. Furthermore, the total volume flowing outward the z -axis is decreased. In table (3.2), the result of effective magnetization parameter on skin-friction coefficient, local Nusselt, boundary layer thickness and volume flowing

outward the z -axis is publicized. It is perceived that with augmentation of magnetization parameter declines, there the shear stress and heat transfer rate at the wall. In the other sundry parameters, displacement thickness is increased because of enrichment in boundary layer thickness due to consequences of magnetization parameter. Furthermore, the total volume flowing outward the z -axis is also increased.

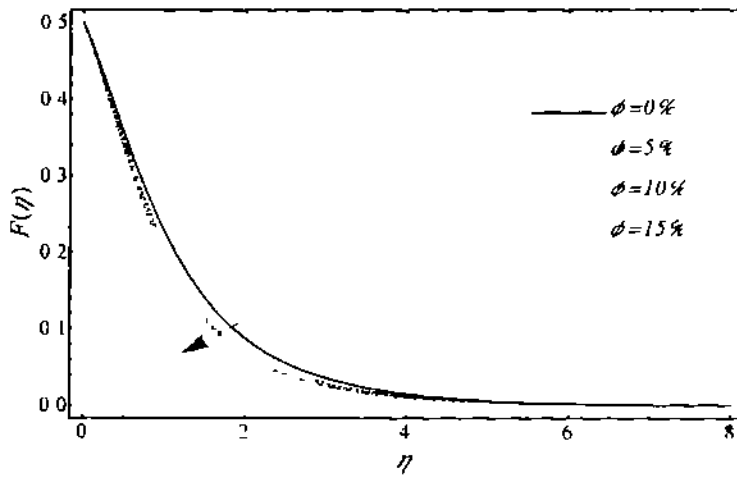


Fig. 3.2: Radial velocity profile for various values of nanoparticle volume fraction

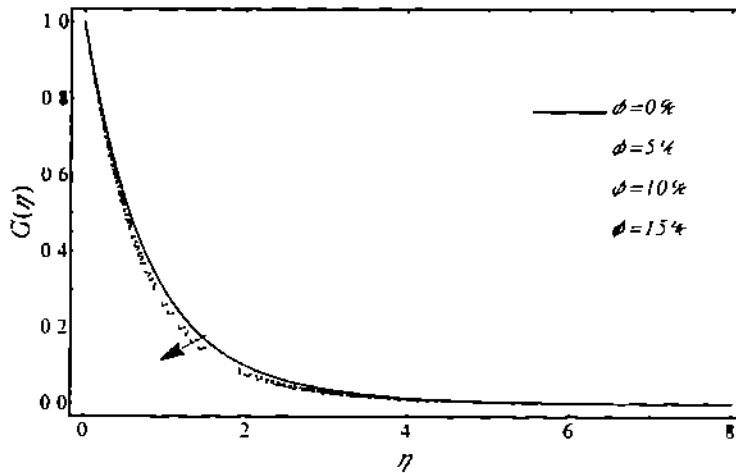


Fig. 3.3: Tangential velocity profile for various values of nanoparticle volume fraction

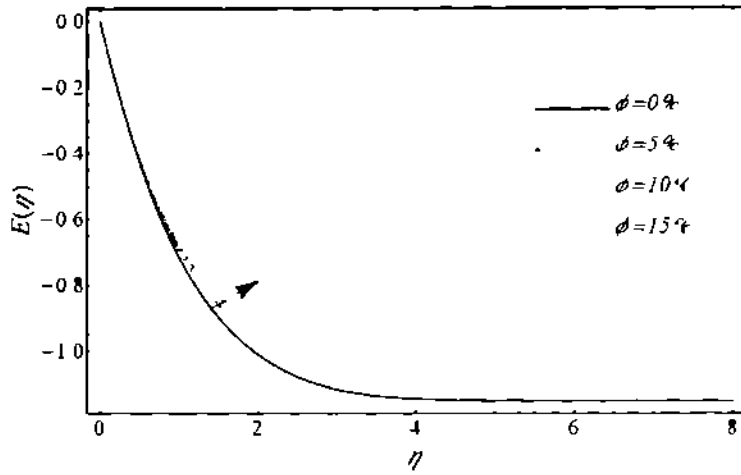


Fig. 3.4: Axial velocity profile for various values of nanoparticle volume fraction

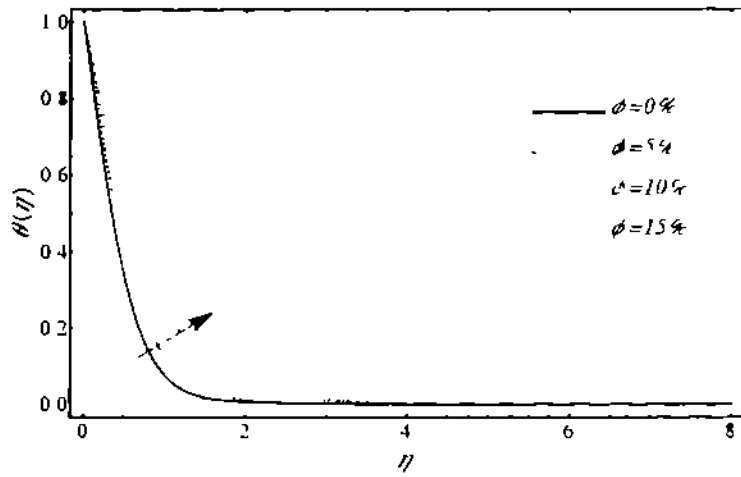


Fig. 3.5: Temperature profile for various values of nanoparticle volume fraction

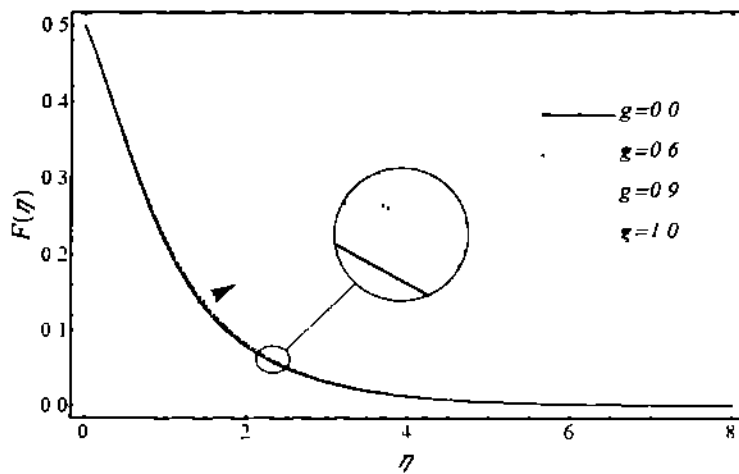


Fig. 3.6: Radial velocity profile for various values of effective magnetization parameter

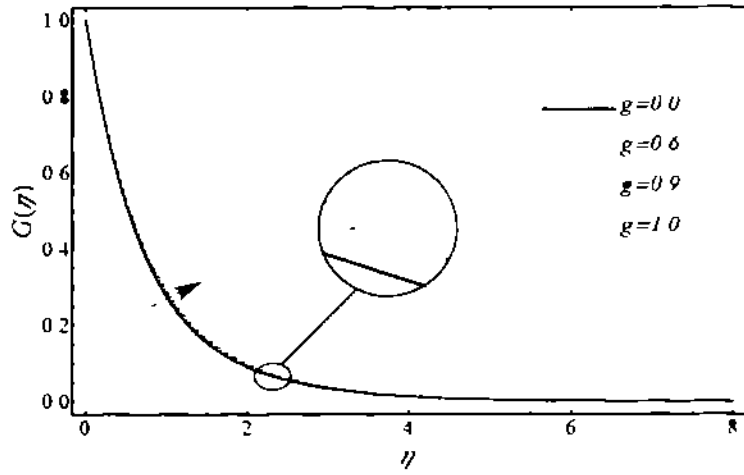


Fig. 3.7: Tangential velocity profile for various values of effective magnetization parameter

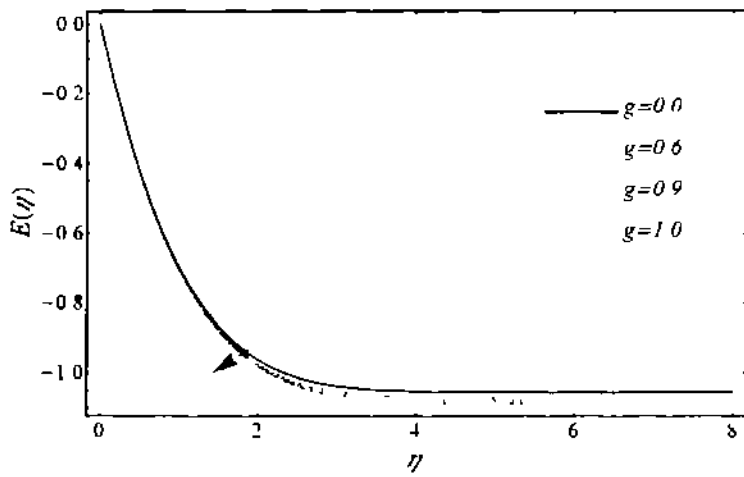


Fig. 3.8: Axial velocity profile for various values of effective magnetization parameter

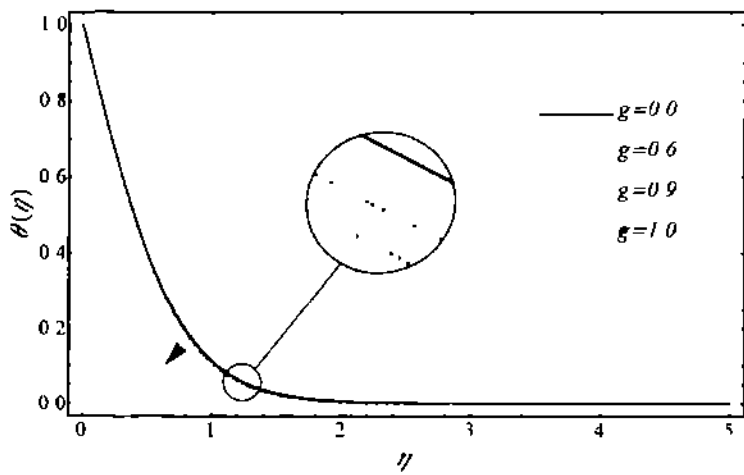


Fig. 3.9: Temperature profile for various values of effective magnetization parameter

Table. 3.1: Values of skin-friction coefficient, local Nusselt, boundary layer thickness, volume flowing outward the z-axis and angle for various values of nanoparticle volume fraction

ϕ	$Re^{1/2} C_f$	$Re^{1/2} Nu$	d	Q
0%	2.5251	1.5891	0.8580	0.6026
5%	3.1222	1.7102	0.7941	0.5591
10%	3.7483	1.8085	0.7628	0.5372
15%	4.4134	1.9174	0.7488	0.5274

Table. 3.2: Values of skin-friction coefficient, local Nusselt, boundary layer thickness, volume flowing outward the z-axis and angle for various values of effective magnetization parameter

g	$Re^{1/2} C_f$	$Re^{1/2} Nu$	d	Q
0	3.1258	1.7097	0.7934	0.5585
0.6	3.0578	1.7194	0.8101	0.5699
0.9	3.0254	1.7239	0.8183	0.5756
01	3.0148	1.7253	0.8210	0.5775

3.4 Concluding remarks

In this chapter, unsteady ferrofluid flow revolving a stretchable rotating disk on a boundary layer is presented. Analytical expressions of velocity and temperature profiles are obtained analytically. The numerical values are found to see the impact of physical parameter g and ϕ on skin friction, Nusselt number, boundary layer thickness and volume flowing through out word the axial-direction through Mathematica wolfram. It is observed that enhancement of ferro-particles concentration changes the physical properties of fluid which distresses the fluid velocity and temperature distribution as well as physical parameters. Both shear stress and heat transfer rate at wall are increased by enrichment of particles concentrations, but boundary layer displacement is decreased. Additionally, it is perceived that with augmentation of magnetization parameter reduces shear stress and heat transfer rate at wall. Moreover, displacement thickness is also increased.

References

- [1] R. P Feynman, R. B Leighton and M. Sands, Lecture on physics, 1 (1963)
- [2] M. I Shliomis, Ferrofluid as thermal ratches, 92 (2004) 18890
- [3] R. E Rosensweig, Ferrohydrodynamic, Cambridge University press, 1985
- [4] V. Karman, Uber laminar and turbulente, Z. Angew. Math. Mech. 1 (1921) 232-252
- [5] H. A. Attia, Unsteady MHD flow near a rotating porous disk with uniform suction or injection. J. Fluid Dynamics Research 23 (1998) 283-290
- [6] K. G. Mithal, On the effect of uniform suction on the steady flow of non-newtonian liquid due to rotating disk, Quart. J. Mech. Appl. Math. 14 (1961) 403-410
- [7] H. A. Attia and A. L. Aboul-Hassan, On hydromagnetic flow due to rotating disk, Appl. Mathematical Modelling 28 (2004) 1007-1014
- [8] P. K. Sunil, Bharti, D. Sharma and R. C. Sharma, The effect of rotation on thermosolutal convection in a ferromagnetic fluid, Int. J. Appl. Mech. and Eng. 10 (2005) 713-730
- [9] S. Venkatasubramanian and P. N. Kaloni, Effect of rotation on the thermos-convective instability of a horizontal layer of ferrofluid, Int. J. Eng. Sci. 32 (1994) 237-256
- [10] M. Das Gupta, and A. S. Convective instability of layer of ferromagnetic fluid rotating about a vertical axis, Int. J. Eng. Sci. 17 (1979) 271-277
- [11] P. Ram and K. Sharma, On the revolving ferrofluid due to rotating disk, Int. J. Non-linear Sci. 13 (2012) 317-324
- [12] S. J. Liao, On the proposed homotopy analysis technique for non-linear problem and its applications, Ph.D. Dissertation, Shanghai Jiao Tong University, 1992
- [13] S. J. Liao, Beyond perturbation, Introduction to homotopy analysis method, Boca Raton, Chapman and Hall/ CRC press, 2003
- [14] S. J. Liao, On the analytic solution of magnetohydrodynamic flow of Non-Newtonian fluids over a stretching sheet, J. Fluid Mech. 488 (2003) 189-212
- [15] S. J. Liao, A new branch of boundary-layer flows over an impermeable stretched plate, Int. J. Heat Mass Transfer 48 (2005) 2529-2539
- [16] S. J. Liao, An analytic solution of unsteady boundary-layer flows caused by an impulsively stretching plate, Comm. Non-linear Sci. Numer. Simul. 11 (2006) 326-339

- [17] H Xu and S J Liao, An analytic solution of magnetohydrodynamic flow of Non-Newtonian fluids caused by an impulsively stretching plate, *J Non-Newtonian Fluid Mech* 42 (2005) 395-405
- [18] Y Tan, H Xu and S J Liao, Explicit series solution of travelling waves of with a front of Fisher equation, *Chaos, Solitons and Fractals* 31 (2007) 462-472
- [19] S Abbasbandy, The application of homotopy analysis method to nonlinear equations arising in heat transfer, *Phys Lett A* 360 (2006) 109-113
- [20] S Abbasbandy, and Z F Samadian, Solution for the fifth-order Kdv equation with homotopy analysis method, *Non-linear Dyne* 51 (2008) 83-87
- [21] R Ellahi, Exact and Numerical solutions for nonlinear differential equation of Jeffrey-Hamel flow, *Int J of Industrial Mathematics* 3 (2011) 1-7
- [22] R Ellahi, A Zeeshan, K Vafai and H U Rehman, Series solutions for magnetohydrodynamic flow of non Newtonian nanofluid and heat transfer in coaxial porous cylinder with slip conditions, *J Nanoengineering and Nanosystems* 225 (2011) 123-132
- [23] P Ram, A Bhandari and K Sharma, Effect of magnetic field-dependent viscosity on revolving ferrofluid, *J Magnetism and Magnetic Materials* 322 (21) (2010) 3476-3480
- [24] W G Cochran, The flow due to rotating disk, *Proc Camb Phil Soc* 30 (1934) 365-375
- [25] E R Benton, On the flow due to rotating disk, *J Fluid Mech* 24 (1966) 781-800
- [26] E Blums, A Cebers and M M Maiorov, *Magnetic Fluids*, Walter de Gruyter, Berlin and New York, 1997
- [27] S Odenbach, *Magneto viscous Effects in Ferrofluids*, Springer-Verlag, Berlin, 2002
- [28] R E Rosensweig, *Ferrohydrodynamics*, Cambridge University Press, 1985
- [29] M I Shliomis and K I Morozov, Negative viscosity of ferrofluid under alternating magnetic field, *Physics of Fluids* 6 (1940) 2855-2861
- [30] P Ram and A Bhandari, Negative viscosity effects on ferrofluid flow due to a rotating disk, *Int J Appl Elect & Mech* 41 (2013) 467-478
- [31] J H Sanchez and C Rinaldi, Magnetoviscosity of dilute suspensions of magnetic ellipsoids obtained through rotational Brownian dynamics simulations, *J of Colloid and Interface Science* 331 (2009) 500-506



/

- [32] M I Shliomis, Ferrohydrodynamics, Testing a third magnetization equation, *Physical Review E* 64 (2001) 060-501
- [33] J C Bacri, R Perzynski, M I Shliomis and G Burde, "Negative-Viscosity" effect in a magnetic fluid, *Physical Review Letters* 75 (1995) 2128-2131
- [34] H Schlichting, *Boundary Layer Theory*, McGraw-Hill Book Company, New York, 1960
- [35] P Ram, A Bhandari and K Sharma, Effect of magnetic field-dependent viscosity on revolving ferrofluid, *J of Magnetism and Magnetic Materials* 322 (2010) 3476-3480
- [36] P Ram and K Sharma, Revolving ferrofluid flow under the influence of MFD viscosity and porosity with rotating disk, *J Electromagnetic Analysis and Applications* 3 (2011) 378-386